Influence of temperature on the optical and luminescent properties of scintillation crystals based on $Gd_3(Ga,Al)_5O_{12}$:Ce

D. Spassky[1,2], N. Krutyak[2,3], A. Ukhanova[3], F. Fedyunin[3], V. Morozov[4], N. Kozlova[5], E. Zabelina[5], V. Kasimova[5], O. Buzanov[6], A. Belik[7]*

Presented at Virtual Session of RAD2021

: Corresponding author e-mail: spas@srd.sinp.msu.ru

Motivation

Ce-doped $Gd_3(Al,Ga)_5O_{12}$ (GAGG) garnets are well-known scintillating crystals for medical applications and high energy physics [1,2]. These crystals attract attention due to the combination of high density, chemical stability, very high light yield and reasonable energy resolution. Recently it was shown that GAGG:Ce crystals with partial substitution of Al and Ga cations by Sc (GASGG:Ce) demonstrate enhanced energy transfer from the host to Ce^{3+} emission centers [3]. The effect results in the increase of light output at low temperatures in GASGG:Ce while at ambient conditions the emission of GASGG:Ce is less intensive due to partial quenching. In the present study we show the influence of temperature on optical and luminescent properties of GAGG:Ce and GASGG:Ce. The composition of the studied crystals was refined using XRD data obtained using synchrotron radiation.

Experimental techniques

Absorption spectra were measured using an Agilent Technologies Cary-5000 spectrophotometer at 300 K and PerkinElmer Lambda 950 spectrophotometer in temperature region 80-500 K.

Luminescence excitation and emission spectra under excitation in the UV region were measured using the laboratory setup based on LOT-Oriel MS257 spectrograph.

The crystal composition of $Gd_3(Ga,Sc,Al)_5O_{12}$

- The single crystals with nominal composition $Gd_{2.97}Ce_{0.03}Ga_3Al_2O_{12}$ (GAGG:Ce) and $Gd_{2.97}Ce_{0.03}Ga_{2.5}Sc_1Al_{1.5}O_{12}$ (GASGG:Ce) were grown by the Czochralski method at the Fomos-Materials (Moscow, Russia, https://newpiezo.com/).
- Synchrotron XRD data for GAGG:Ce and GASGG:Ce were measured in a large Debye–Scherrer camera at the BL15XU beamline of SPring-8.

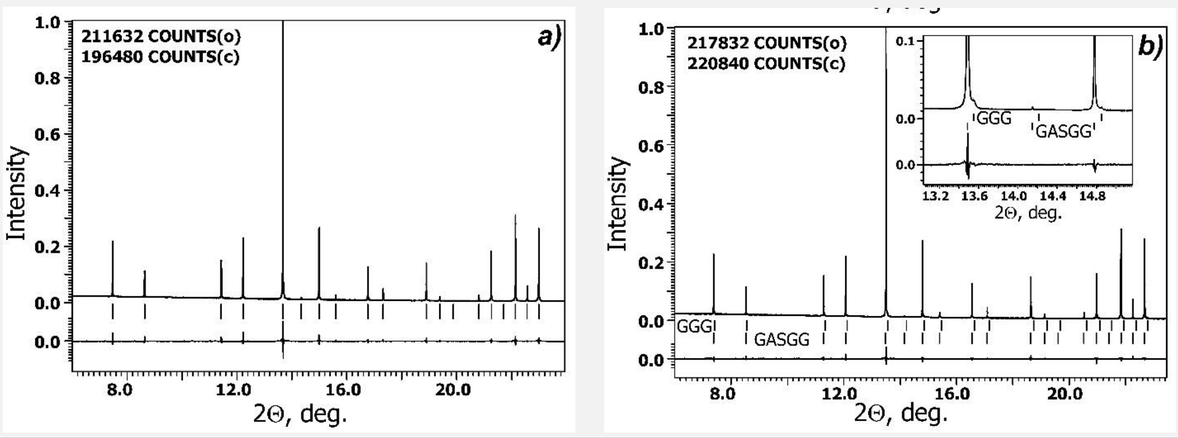

Figure 1. Fragments of the observed, calculated and difference XRD patterns for $Gd_3Al_{2.22}Ga_{2.78}O_{12}$:Ce (*a*) and $Gd_{2.08}Sc_{1.99}Al_{2.90}Ga_{1.03}O_{12}$:Ce (*b*). Tick marks denote the peak positions of possible Bragg reflections. The inset shows the part of the XRD patterns in 2*Q* range of 13-15.2°.

- GAGG has cubic structure with a space group of *Ia3d*;
- The general chemical formula $A_3B_2{}^{oct}C_3{}^{tet}O_{12}$ contains three types of oxygen polyhedrons;
- According to the performed refinement of crystal structure it was shown that dodecahedral sites are occupied by Gd^{3+} ions in GAGG and Gd^{3+}/Sc^{3+} in GASGG while octahedral sites are occupied by Ga^{3+}/Al^{3+} in GAGG and Al^{3+}/Sc^{3+} in GASGG and tetrahedral sites are occupied by Ga^{3+}/Al^{3+} in both crystals .
- Ga^{3+} ions prefer to occupy tetrahedral sites in GAGG due to higher covalency rate in comparison to Al^{3+}.

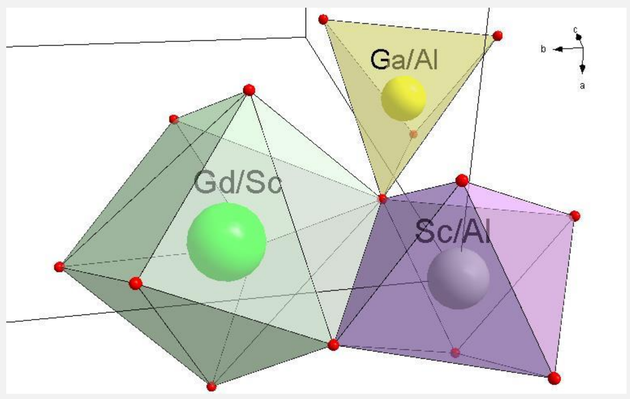

	Atom	x	y	z	U_{iso}	Occupancy
GAGG	A	0.125	0	0.25	0.0071(4)	Gd^{3+}
	B	0	0	0	0.0076(14)	0.400(7) Ga^{3+}
						0.660(7) Al^{3+}
	C	0.375	0	0.25	0.0042(12)	0.605(5) Ga^{3+}
						0.340(5) Al^{3+}
	O	0.2791(3)	-0.1009(3)	0.3002(3)	0.0001(15)	O
GASGG	A	0.125	0	0.25	0.0057(3)	0.69(2) Gd^{3+}
						0.31(2) Sc^{3+}
	B	0	0	0	0.001(2)	0.54(4) Sc^{3+}
						0.46(4) Al^{3+}
	C	0.375	0	0.25	0.0002(11)	0.34(2) Ga^{3+}
						0.66(2) Al^{3+}
	O	0.2819(2)	-0.0964(2)	0.3050(2)	0.055(4)	O

Table 1. Fractional atomic coordinates, site symmetry, isotropic displacement atomic parameters (U_{iso}) and site occupation for $Gd_3Al_{2.22}Ga_{2.78}O_{12}$ and $Gd_{2.08}Sc_{1.99}Al_{2.90}Ga_{1.03}O_{12}$.

Optical properties of $Gd_3(Ga,Sc,Al)_5O_{12}$

1. Absorption spectra

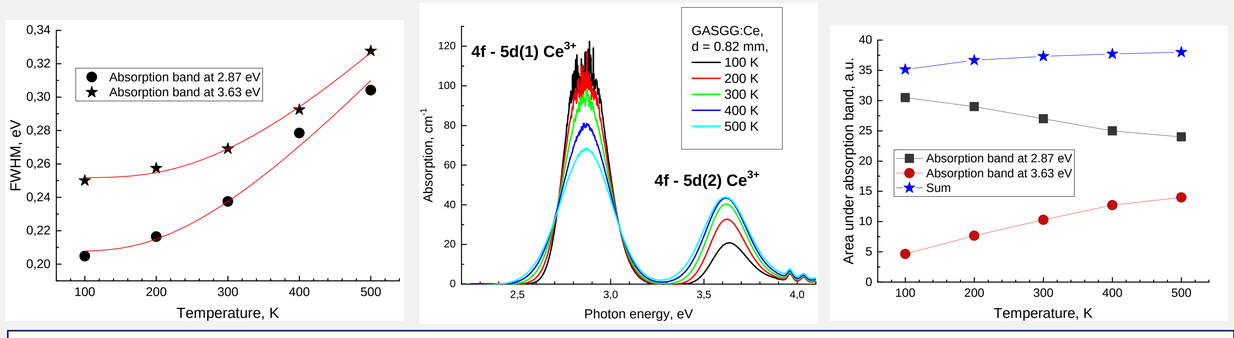

Figure 2. Temperature dependences of absorption spectra (at center), FWHM of the absorption bands (at left) and area under absorption bands (at right) of GASGG single crystal. Fit of FWHM dependences using formula (1) is represented by thin red lines.

- Redistribution of intensities of absorption bands which arise due to 4f – 5d(1) and 5d(2) Ce^{3+} transitions is related to thermal population of high-energy sub-level of $^2F_{5/2}$ ground state. The latter is split into three levels due to spin-orbit interaction.
- The absorption bands broadens with temperature due to electron-phonon interaction. The temperature dependence of FWHM can be fit using formula (1). The phonon energies of parabolas, which describe ground and excited states of Ce^{3+} were obtained as a result and presented in Table 1.

2. Luminescence spectra

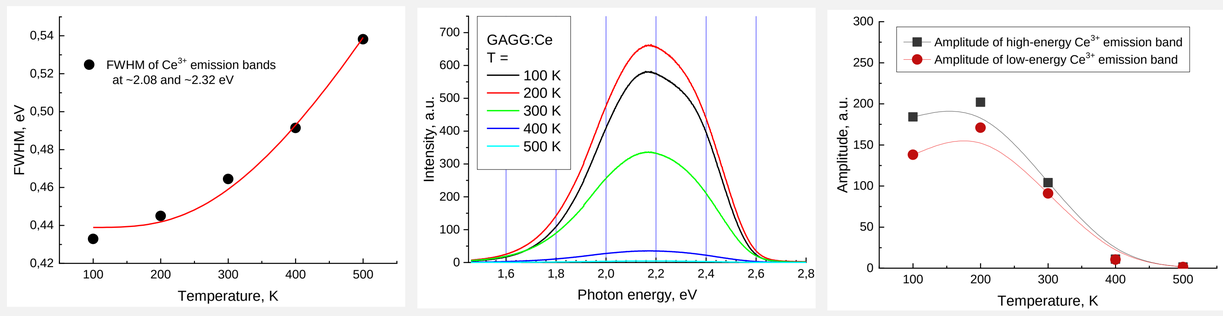

Figure 3. Temperature dependences of luminescence spectra (at center), FWHM of the emission bands (at left) and area under emission bands (at right) of GAGG single crystal. Fit of FWHM dependences using formula (1) is represented by thin red line.

- The luminescence spectra of both studied crystals consists of two strongly overlapped emission bands, which arise due to 5d(1) – $^2F_{7/2}$, $^2F_{5/2}$ transitions in Ce^{3+}. The spectra were fit using the sum of two Gaussians with equal FWHM parameters and difference between the emission peaks 0.24 eV, which correspond to the energy gap between $^2F_{7/2}$ and $^2F_{5/2}$.
- The amplitudes decreases with temperature due to thermal quenching of Ce^{3+} emission.
- The emission bands broadens with temperature due to electron-phonon interaction similarly to the absorption bands. The fit using (1) has been also performed for the temperature dependence of FWHM and the phonon energies $\hbar\Omega_0$ and $\hbar\Omega_1$ were obtained as a result and presented in Table 1.

3. The model

- The shape of the absorption and emission lines can be described using formulas

$$G_{abs}(\hbar\omega) = \frac{1}{\sqrt{2\pi}\,\Delta_{abs}(T)} \exp\left[-\frac{(\hbar\omega - E_{abs})^2}{2\Delta_{abs}^2(T)}\right]$$

$$G_{em}(\hbar\omega) = \frac{1}{\sqrt{2\pi}\,\Delta_{em}(T)} \exp\left[-\frac{(\hbar\omega - E_{em})^2}{2\Delta_{em}^2(T)}\right]$$

- The temperature dependence of FWHM is given formulas:

$$\Delta_{abs}^2(T) = \frac{(E_{abs} - E_{em})(\hbar\Omega_1)^4 \operatorname{cth}(\hbar\Omega_0/2k_BT)}{\hbar\Omega_0\left((\hbar\Omega_0)^2 + (\hbar\Omega_1)^2\right)}$$

$$\Delta_{em}^2(T) = \frac{(E_{abs} - E_{em})(\hbar\Omega_0)^4 \operatorname{cth}(\hbar\Omega_1/2k_BT)}{\hbar\Omega_1\left((\hbar\Omega_0)^2 + (\hbar\Omega_1)^2\right)}$$

	Experiment	Absorption		Luminescence	
	Crystal	GAGG	GASGG	GAGG	GASGG
Low-energy band	$\hbar\Omega_0$, meV	45	59	142	170
	$\hbar\Omega_1$, meV	75	97	60	68
High-energy band	$\hbar\Omega_0$, meV	50	40	-	-
	$\hbar\Omega_1$, meV	54	47	-	-

, where E_{abs}, E_{em} – maxima of absorption and emission bands, T –temperature, k_B – Boltzman constant, $\hbar\Omega_0$ and $\hbar\Omega_1$ – phonon energies of the ground state and excited state. The latter values determines the slope of ground state and excited state parabolas in the model of configurational curves.

Conclusions

- The composition of GAGG:Ce and GASGG:Ce was refined using XRD data obtained using synchrotron radiation. It is shown that Sc cations distributed between dodecahedral and octahedral sites. Ga cations are preferably occupies octahedral sites.
- The influence of temperature on absorption and luminescence spectra of the studied crystals was shown. The fit of temperature dependencies of FWHM of absorption and emission peaks was performed. The phonon energies $\hbar\Omega_0$ and $\hbar\Omega_1$ were obtained as a result of fitting. Different FWHM of the absorption and emission bands arise due to non-equivalent values of $\hbar\Omega_0$ and $\hbar\Omega_1$.

Acknowledgements

The research was supported by Russian Foundation for Basic Research №20-02-00688.

Affiliation of the authors

[1]*Skobeltsyn Institute of Nuclear Physics, M.V. Lomonosov Moscow State University, Russia*
[2]*Institute of Physics, University of Tartu, Estonia*
[3]*Physical Department, M.V. Lomonosov Moscow State University, Russia*
[4]*Chemistry Department, M.V. Lomonosov Moscow State University, Russia*
[5]*National University of Science and Technology (MISiS), Moscow, Russia*
[6]*Fomos-Materials, Moscow, Russia*
[7]*International Center for Materials Nanoarchitectonics (WPI-MANA), National Institute for Materials Science, Namiki 1-1, Tsukuba, Ibaraki 305-0044, Japan*